Properties of $(Nb_{0.35}, Ti_{0.15})_xNi_{1-x}$ thin films deposited on silicon wafers at ambient substrate temperature

N. N. Iosad[a)]
Delft University of Technology, Department of Applied Physics (DIMES), Lorentzweg 1, 2628 CJ Delft, The Netherlands

A. V. Mijiritskii
University of Groningen, Nuclear Solid State Physics, Nijenborgh 4.13, 9747 AG Groningen, The Netherlands

V. V. Roddatis
Institute of Crystallography Russian Academy of Sciences, Leninsky pr. 59, 117333 Moscow, Russia

N. M. van der Pers
Delft University of Technology, Laboratory for Materials Science, Rotterdamseweg 137, 2628 AL Delft, The Netherlands

B. D. Jackson and J. R. Gao
Space Research Organization of the Netherlands, P.O. Box 800, 9700 AV Groningen, The Netherlands

S. N. Polyakov
Institute of Nuclear Physics, Moscow State University, 119899, GSP, Moscow, Russia

P. N. Dmitriev
Institute of Radioelectronics Russian Academy of Sciences, Mokhovaya 11, 103907, GSP-3, Moscow, Russia

T. M. Klapwijk
Delft University of Technology, Department of Applied Physics (DIMES), Lorentzweg 1, 2628 CJ Delft, The Netherlands

(Received 16 May 2000; accepted for publication 24 August 2000)

We have studied the properties of $(Nb_{0.35}, Ti_{0.15})_xN_{1-x}$ films deposited by reactive magnetron sputtering at ambient substrate temperature, focusing in particular on the dependence of film properties on the total sputtering pressure. As the pressure increases we observe a transition in the film structure from the ZT to the Z1 structural zone according to the Thornton classification. In general, the superconducting transition temperature (T_c) and residual resistance ratio have a very moderate dependence on total sputtering pressure, while the film resistivity increases an order of magnitude as the sputtering pressure increases. A wide spectrum of material science techniques is used to characterize the films and to explain the relationship between the sputtering conditions and film properties. Transmission electron microscopy and x-ray diffraction analysis show that 160-nm-thick $(Nb_{0.35}, Ti_{0.15})_xN_{1-x}$ films consist of 20–40 nm grains with good crystallinity. Films sputtered under low pressures have a weak [100] texture, while films sputtered under high pressures have a distinct [111] texture. A stable chemical composition and reduction in film density as the sputtering pressure increases indicate that the change of resistivity in the ZT structural zone is due to a variation in the quenched-in vacancy concentration. In contrast voids on the grain boundaries and vacancies together produce the high film resistivities in the Z1 structural zone. © *2000 American Institute of Physics.* [S0021-8979(00)02723-7]

INTRODUCTION

The fundamental limitation of Nb striplines, according to Mattis–Bardeen theory, is determined by the Nb gap frequency (≈700 GHz).[1] For this reason the development of superconductor–insulator–superconductor (SIS) tetrahertz (THz) detectors based on Nb/Al–AlO_x/Nb junctions requires that other materials such as Al,[2,3] Nb_xN_{1-x},[4] and $(Nb, Ti)_xN_{1-x}$ (Refs. 5, 6) can be used for the striplines. $(Nb, Ti)_xN_{1-x}$ films have been used for thin-film coated rf cavities for high-energy accelerators[7] and, more recently, have been introduced as a tuning circuit material for SIS mixers. The primary advantage of this material over Nb_xN_{1-x} and Al is that it is a relatively low-loss superconductor with a frequency gap comparable to the maximum operating frequency of a Nb SIS junction, ~1.2 THz.[8] Thus, it is hoped that the integration of $(Nb, Ti)_xN_{1-x}$ striplines with Nb SIS junctions will enable the development of low noise SIS receivers in the 0.8–1.2 THz frequency range.

Because the normal state resistivity of a conventional superconducting film provides a good estimate of rf losses in the film, our research focuses on obtaining low resistivity $(Nb, Ti)_xN_{1-x}$ films, while maintaining all other film prop-

a)Electronic mail: iosod@dimes.tudelft.nl

erties appropriate for the integration of $(Nb, Ti)_xN_{1-x}$ striplines with Nb SIS junctions. An understanding of the technological factors determining the film quality, combined with a detailed material study, will provide a platform for further improvement of the films and for predicting their behavior at THz frequencies. Various techniques are used for the deposition of nitrides, including dc and rf reactive sputtering,[9,10] ion-beam deposition,[11] reactive evaporation,[12] pulsed laser deposition,[13] and magnetron sputtering.[5,14–16] Because dc and rf magnetron sputtering are two of the most promising methods for device fabrication, we focus on this method in our work.

In general, the properties of $(Nb, Ti)_xN_{1-x}$ and similar materials like Nb_xN_{1-x} or Ti_xN_{1-x} show a strong dependence on the magnetron sputtering conditions. An increase in the substrate surface temperature by intentional heating, changing thermalization conditions of the sputtering yield by total sputtering pressure, or applying a substrate bias, results in a reduction of the resistivity, a change in the texture from [111] to [100], and an increase in T_c.[17–19] In this article we compare the properties of the films sputtered under different total pressures with a particular focus on the strong dependence of film resistivity on sputtering pressure. Two different concepts have been proposed to explain the origin of high resistivities in carbides and nitrides of transition metals. Toth explains this effect by a high concentration and high degree of disorder of vacancies at both metal and nonmetal sites.[17,20] While Bacon *et al.* state that the high resistivity of magnetron sputtered Nb_xN_{1-x} films is due to voids on the grain boundaries.[21] In this article we show that both mechanisms can play a role in determining the resistivity of $(Nb, Ti)_xN_{1-x}$ films depending upon the sputtering conditions used.

EXPERIMENT

Films of $(Nb_{0.35}, Ti_{0.15})_xN_{1-x}$ are deposited by reactive magnetron sputtering in a Nordiko-2000 sputtering system with a base pressure of 4×10^{-5} Pa. This sputtering machine is equipped with a cryopump and a throttling valve, which together determine the process pressure, while the injection of Ar and N_2 gases is controlled by flow meters. In order to avoid the hysteretic sputtering regime, the pumping rate is fixed at a high value of 750 l/s for all experiments.[22] A 99.8% pure alloy target with 30 at. % Ti and 70 at. % Nb is used. All films are sputtered with 300 W dc power, resulting in a deposition rate of 80 ± 10 nm/min. Wafers are fixed to the copper chuck with diffusion pump oil to stabilize the thermodynamics of growth. In order to maximize film uniformity, the substrate-target distance is set to the maximum for our sputtering system, 8 cm.

Films (160 ± 10 nm thick) sputtered on silicon wafers were used for T_c, resistivity, x-ray diffraction (XRD), room temperature Hall coefficients, density, and intrinsic stress measurements. The stress in the films is evaluated measuring the deflection of the wafer before and after film deposition with a profilometer. Assuming that the film thickness is much less than the substrate thickness, the film stress is then calculated using Stoney's equation

$$\sigma=\frac{1}{6R}\frac{E}{(1-\nu)}\frac{D^2}{d},$$

where E, v, and D are the Young's modulus, Poisson's ratio, and thickness of the substrate, respectively. $E/(1-\mathrm{v})$ equals to 181 GPa for Si [100], d is the film thickness, and R is the radius of curvature of the substrate, calculated from the deflection measurement.[23,24] T_c is evaluated from the dependence of film resistivity on temperature. Film density is determined form the weight of the layer. The Hall coefficient is measured using standard Hall voltage measurement.

The chemical composition of the films is measured by Rutherford backscattering spectroscopy (RBS) using 1 MeV He^+ beam for sample irradiation. The backscattered particles are detected at an angle of 165°, and the measurements are done in an UHV chamber with a base pressure of 5×10^{-6} Pa. A ''random'' RBS spectrum is obtained by summing up the RBS spectra acquired during a 360° RBS azimuthal scan measurements with a 10° beam incidence off the surface normal. A detailed analysis of the measured RBS spectra is performed by the ''RUMP'' program. Relatively thin films (50 nm) sputtered on Si wafers are used for this kind of analysis in order to allow the scaling onto the substrate yield in the RBS simulation routine. We expect that the nitrogen content does not depend on the film thickness, because the chemical composition is determined by the nitration of the cathode, rather than by processes taking place on the film surface.[25] Thus, the RBS data on the chemical composition of the thin films should be valid also for thicker samples. Note that RBS also revealed that the level of possible contaminants (such as oxygen and carbon) in all films is below 1 at. %.

XRD Θ–2Θ scans in the 2Θ range from 20° to 125° are performed using a Rigaku D/max-Rc diffractometer equipped with a 12 kW x-ray generator of Cu$K\alpha$ radiation and a graphite crystal monochromator. XRD texture measurements are performed with a Bruker-AXS D5005 diffractometer equipped with a Huber Eulerian Cradle, also using Cu $K\alpha$ radiation. The specimen tilt-angle range is 0°–80° with a step size of 10°. 2Θ range was selected from 32° to 45° to monitor to most intensive [111] and [200] reflections. Integral reflection intensity was used for the texture analysis. Plan-view samples are prepared by a standard technique—mechanical thinning down to 30 μm and followed by ion milling using a Gatan 600 duo ion mill. The specimens are examined with a Philips EM430ST transmission electron microscope operated at 200 kV.

RESULTS AND DISCUSSION

We have optimized the nitrogen injection for the wide range of total sputtering pressures in order to have maximum T_c of the $(Nb_{0.35}, Ti_{0.15})_xN_{1-x}$ films. The limits of the pressure range are determined by film degradation caused by destructive bombardment of the growing film by the fast neutrals at low pressures and high thermalization conditions at high pressures.[26] Figure 1 illustrates the dependence of film properties versus total sputtering pressure. T_c, and the Hall coefficient are weakly dependent on pressure, film resistivity increases strongly while compressive stress de-

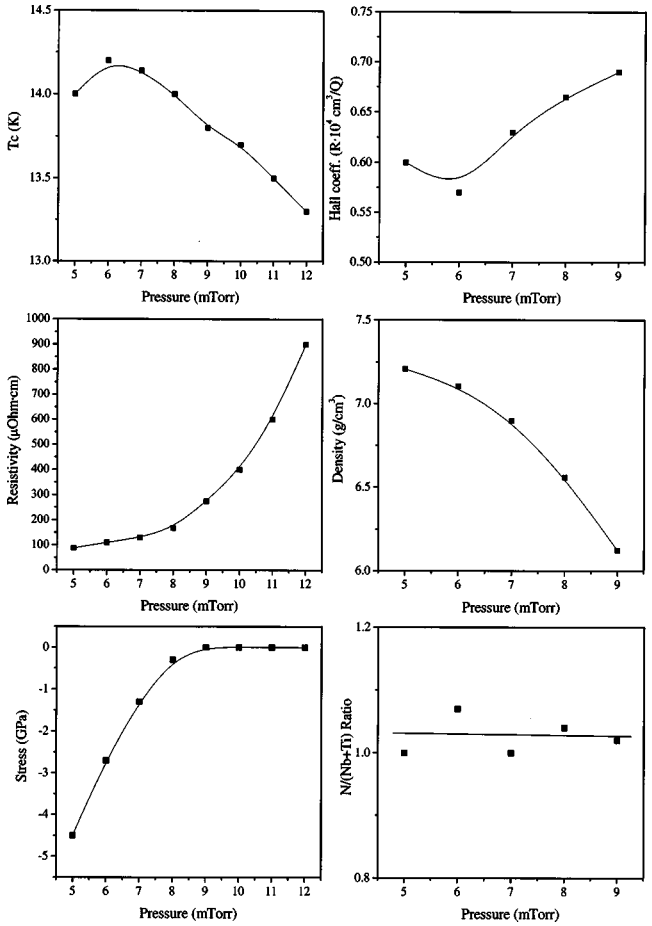

FIG. 1. Transition temperature, Hall coefficient, film resistivity, film density, intrinsic stress, and chemical composition of the $(Nb_{0.35}, Ti_{0.15})_xN_{1-x}$ films sputtered under different pressures.

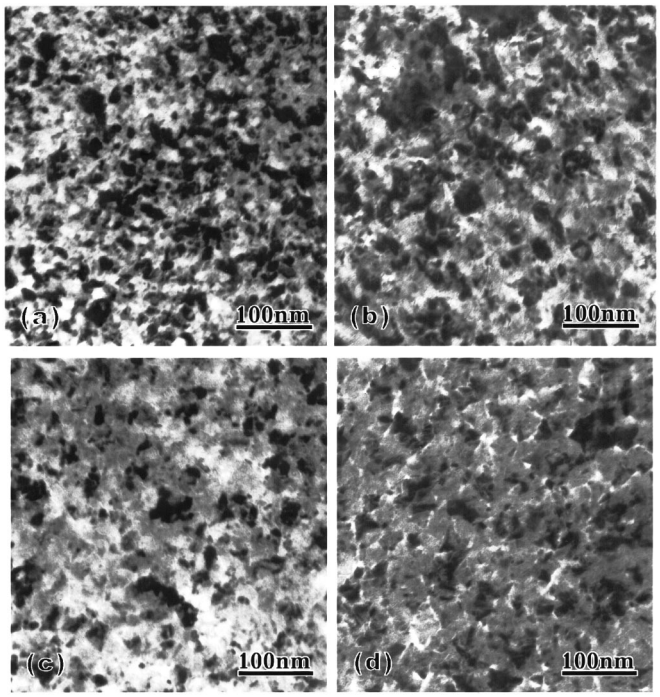

FIG. 2. Plan views TEM images of the $(Nb_{0.35}, Ti_{0.15})_xN_{1-x}$ films deposited under different sputtering pressures (5, 7, 9, and 12 mTorr) pictures (a)–(d) correspondingly.

creases strongly with increasing pressure. Film density decreases with increasing pressure. The chemical composition is almost the same for different sputtering pressures.

We can define two separate structure zones of the $(Nb_{0.35}, Ti_{0.15})_xN_{1-x}$ films versus sputtering pressure according to Thornton classification.[27,28] Films sputtered in the pressure range of 5–9 mTorr belong to the ZT structural zone, since they are in a state of compressive stress and XRD analysis shows numerous peaks in the Θ–2Θ scans, i.e., there is no strong texture present (Table I). A further increase in the sputtering pressure results in a flattening of the stress curve at $\approx$0 GPa. This allows to attribute the films sputtered in the pressure range of 10–12 mTorr to the Z1 structural zone. According to Thornton films in the ZT structural zone have tight grain boundaries, while the films in the Z1 structural zone have voids on the grain boundaries. Those results are in good correlation with the data obtained by the transmission electron microscopy (TEM). Figure 2 illustrates several plan views of the films sputtered under different pressures. Only the film belonging to Z1 structural zone have white regions at the grain boundaries, which could be voids or thick layers of amorphous material, while all other films shown on the Fig. 2 have tight grain boundaries.

Since we are interested in low-resistivity films we will focus further discussion on the films belonging to the ZT structural zone. In particular, noting that the measured T_c and Hall coefficient have a relatively moderate dependence on sputtering pressure, when compared with the change in resistivity, we conclude that the variation of the resistivity is not determined by changes in the density of states at the Fermi level. Furthermore observation of a steady nitrogen concentration (slightly exceeding 50 at. %) and the increase in film density with the decrease of sputtering pressure gives us a clear indication that there is a variation in the quenched-in vacancy concentration in the films. Because the sputtering pressure controls the heat flux towards the substrate by the thermalization of fast neutrals and the particles

TABLE I. Θ–2Θ XRD patterns of the $(Nb_{0.35}, Ti_{0.15})_xN_{1-x}$ films sputtered under different total pressures.

	Relative top intensities for different total pressures							
hkl	5 mTorr	6 mTorr	7 mTorr	8 mTorr	9 mTorr	10 mTorr	11 mTorr	12 mTorr
111	45	100	100	100	100	100	100	100
200	100	95	36	26	19	12	11	9
220	21	38	14	9	9	8	8	7
311	20	25	13	8	6	6	6	5

of the sputtering yield, we explain this increase in the vacancy concentration by a reduction of surface diffusion as the sputtering pressure increases.[29]

Since increase of conductivity and compressive stress are in good correlation in the ZT structural zone, it is interesting to discuss an alternative mechanism for the observed vacancy concentration variation. In particular annealing of Ti_xO_{1-x} samples under pressures $\approx$0.01 GPa results in a considerable reduction of the vacancy concentration.[30] During magnetron sputtering we have similar conditions for the film layers close to the surface of the film. High temperature is produced by plasma heating and high pressure is created by intrinsic stress in the $(Nb_{0.35}, Ti_{0.15})_xN_{1-x}$ film. However, our experiments show that the intrinsic stress in the films also depends on film thickness and glow discharge type, while film resistivity is determined exclusively by pressure. Thus, we conclude that intrinsic stress has a minimal effect on film resistivity, and that film resistivity is determined exclusively by the thermalization conditions in the glow discharge.

High vacancy concentration and high degree of disorder can modify the x-ray scattering amplitudes and, as a consequence, change the XRD reflections intensity. In order to determine the significance of this effect we have performed Θ–2Θ scans with different specimen inclination angles in the Ψ direction for films sputtered under pressures of 6 and 9 mTorr. Data analysis showed that the film sputtered under 6 mTorr pressure has a weak [100] texture and compressive stress, while the film sputtered under 9 mTorr pressure is almost stress-free and has a distinct [111] texture. Thus, the observed changes of the x-ray patterns summarized in the Table I are mainly due to different textures present in the films. Similar changes in texture as a result of intentional heating were previously observed for Ti_xN_{1-x} films.[31] Moreover, the artificial initiation of [100] texture by sputtering on a MgO underlayer results in considerable reduction of resistivity and slight increase of T_c in Nb_xN_{1-x} films.[32] These results are in good correlation with our observations, since in our case we initiate the same changes in texture ([111] to [100]) by reducing the sputtering pressure to elevate the substrate surface temperature.

CONCLUSIONS

The structural and electrical properties of $(Nb_{0.35}, Ti_{0.15})_xN_{1-x}$ films are examined over a wide range of sputtering pressures. The films consist of 20–40 nm grains with good crystallinity. Films sputtered under low pressures have a weak [100] texture, while films sputtered under high pressures have a distinct [111] texture. We observe a change of the film structure from the Z1 structural zone to the ZT structural zone as the sputtering pressure decreases. T_c has a moderate dependence on the sputtering pressure, while film resistivity increases one order of magnitude as the pressure increases. Because all of our films have residual resistance ratios in the vicinity of unity, we conclude that the origin of high resistivities is related to crystal imperfections. In particular, film resistivity is determined by vacancies in the ZT structural zone, while the voids on the grain boundaries and vacancies together determine the resistivity in the Z1 structural zone. Further improvement of the film properties is limited by destructive bombardment of the fast neutrals, thus alternative means have to be used such as utilization of MgO wafers or sputtering at elevated substrate temperature.

ACKNOWLEDGMENTS

The authors thank B. Wolfs, S. Bakker, E. K. Kov'ev, V. P. Koshelets, F. D. Tichelaar, A. H. Verbruggen, and R. Delhez for helpful discussions and assistance in experimental work. The work was supported in parts by INTAS Project No. 97-1712, ISTC Project No. 1199, and ESA Contract No. 11653/95.

[1] D. C. Mattis and J. Bardeen, Phys. Rev. **111**, 412 (1958).
[2] H. van de Stadt *et al.*, Proceedings of the 6th International Symposium On Space Terahertz Technology, CIT, PC, 1995, p. 66.
[3] M. Bin, M. C. Gaidis, J. Zmuidzinas, T. G. Phillips, and H. G. Leduc, Appl. Phys. Lett. **68**, 1714 (1996).
[4] Y. Uzawa, Z. Wang, and A. Kawakami, Proceedings of the 9th International Symposium on Space Terahertz Technology, CIT, PC, 1998, p. 273.
[5] J. Kawamura, J. Chen, D. Miller, J. Kooi, J. Zamudzinas, B. Blumble, H. G. LeDuc, and J. A. Stern, Appl. Phys. Lett. **75**, 4013 (1999).
[6] B. Jackson, N. Iosad, W. Laauwen, G. de Lange, J. Gao, H. van de Stadt, and T. Klapwijk, Proceedings of the 9th International Symposium on Space Terahertz Technology, Charlottesville, Virginia, 1999, p. 144.
[7] R. Di Leo, A. Nigro, G. Nobile, and R. Vaglio, J. Low Temp. Phys. **78**, 41 (1990).
[8] A. Stern, B. Blumble, H. LeDuc, W. J. Kooi, and J. Zmuidzinas, Proceedings of the 9th International Symposium on Space Terahertz Technology, CIT, PC, 1997, p. 305.
[9] J. R. Gavaler, J. Vac. Sci. Technol. **18**, 247 (1981).
[10] M. E. Gershenzon and V. P. Koshelets, Sov. Phys. Tech. Phys. **25**, 343 (1980).
[11] K. Takei and K. Nagai, Jpn. J. Appl. Phys. **20**, 993 (1981).
[12] A. Sterling, J. Appl. Phys. **20**, 993 (1981).
[13] R. E. Treece, J. S. Horowitz, J. H. Claassen, and B. Chrisey, Appl. Phys. Lett. **65**, 2860 (1994).
[14] N. N. Iosad, B. D. Jackson, T. M. Klapwijk, S. N. Polyakov, P. N. Dmitriev, and J. R. Gao, IEEE Trans. Appl. Supercond. **9**, 1716 (1999).
[15] A. Shoji, IEEE Trans. Magn. **27**, 3184 (1991).
[16] Y. Uzawa, Z. Wang, and A. Kawakami, Proceedings of the 9th International Symposium on Space Terahertz Technology, CIT, PC, 1998, p. 273.
[17] N. Savvides and B. Window, J. Appl. Phys. **64**, 225 (1988).
[18] N. N. Iosad, T. M. Klapwijk, S. N. Polyakov, V. V. Roddatis, E. K. Kov'ev, and P. N. Dmitriev, IEEE Trans. Appl. Supercond. **9**, 1720 (1999).
[19] N. N. Iosad, B. D. Jackson, F. Ferro, J. R. Gao, S. N. Polyakov, P. N. Dmitriev, and T. M. Klapwijk, Semicond. Sci. Technol. **12**, 736 (1999).
[20] L. E. Toth, *Transition Metal Carbides and Nitrides* (Academic, New York, 1971), p. 190.
[21] D. D. Bacon, A. T. English, S. Nakahara, F. G. Peters, H. Schreiber, W. R. Sinclair, and R. B. van Dover, J. Appl. Phys. **54**, 6509 (1983).
[22] K. L. Westra, M. J. Brett, and J. F. Vaneldik, J. Vac. Sci. Technol. A **8**, 1288 (1990).
[23] W. A. Brantley, J. Appl. Phys. **44**, 534 (1973).
[24] G. C. Stoney, Proc. R. Soc. London, Ser. A **32**, 172 (1909).
[25] J. Brchka and I. Hotovy, Vacuum **46**, 1407 (1995).
[26] M. Wittmer, J. Vac. Sci. Technol. A **3**, 1797 (1985).
[27] D. L. Smith, *Thin Film Deposition* (McGraw-Hill, New York, 1995), p. 160.
[28] D. L. Smith, *Thin Film Deposition* (McGraw-Hill, New York, 1995), p. 197.
[29] K.-H. Muller, J. Appl. Phys. **62**, 1796 (1987).
[30] N. J. Doyle, J. K. Hulm, C. K. Jones, R. C. Miller, and A. Taylor, Phys. Lett. **26A**, 604 (1968).
[31] Q. Wang, T. Kikuchi, S. Kohijro, and A. Shoji, IEEE Trans. Appl. Supercond. **7**, 2801 (1997).
[32] J. C. Villegier, M. Radparvar, L. S. Yu, and S. M. Faris, IEEE Trans. Magn. **25**, 1227 (1989).